

Intracellular pH Measurements Using Perfluorocarbon Nanoemulsions

Michael J. Patrick,[†] Jelena M. Janjic,[‡] Haibing Teng,[†] Meredith R. O'Hear,^{§,#} Cortlyn W. Brown,^{||,∇} Jesse A. Stokum,[§] Brigitte F. Schmidt,[†] Eric T. Ahrens,^{*,§,⊥,||} and Alan S. Waggoner[†]

[†]Molecular Biosensor and Imaging Center, Carnegie Mellon University, Pittsburgh, Pennsylvania 15213, United States

[‡]Graduate School of Pharmaceutical Sciences, Duquesne University, Pittsburgh, Pennsylvania 15219, United States

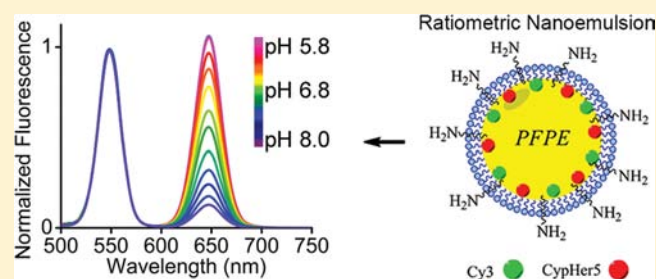
[§]Department of Biological Sciences, Carnegie Mellon University, Pittsburgh, Pennsylvania 15213, United States

^{||}Department of Biological Sciences, University of Chicago, Chicago, Illinois 60637, United States

[⊥]Pittsburgh NMR Center for Biomedical Research, Carnegie Mellon University, Pittsburgh, Pennsylvania 15213, United States

Supporting Information

ABSTRACT: We report the synthesis and formulation of unique perfluorocarbon (PFC) nanoemulsions enabling intracellular pH measurements in living cells via fluorescent microscopy and flow cytometry. These nanoemulsions are formulated to readily enter cells upon coinubation and contain two cyanine-based fluorescent reporters covalently bound to the PFC molecules, specifically Cy3-PFC and CypHer5-PFC conjugates. The spectral and pH-sensing properties of the nanoemulsions were characterized *in vitro* and showed the unaltered spectral behavior of dyes after formulation. In rat 9L glioma cells loaded with nanoemulsion, the local pH of nanoemulsions was longitudinally quantified using optical microscopy and flow cytometry and displayed a steady decrease in pH to a level of 5.5 over 3 h, indicating rapid uptake of nanoemulsion to acidic compartments. Overall, these reagents enable real-time optical detection of intracellular pH in living cells in response to pharmacological manipulations. Moreover, recent approaches for *in vivo* cell tracking using magnetic resonance imaging (MRI) employ intracellular PFC nanoemulsion probes to track cells using ¹⁹F MRI. However, the intracellular fate of these imaging probes is poorly understood. The pH-sensing nanoemulsions allow the study of the fate of the PFC tracer inside the labeled cell, which is important for understanding the PFC cell loading dynamics, nanoemulsion stability and cell viability over time.



1. INTRODUCTION

Measurement of real-time intracellular pH is useful in the development of intracellular drug delivery systems and *in vitro* pharmacology studies. A common uptake mechanism of protein and nanoreagent delivery involves endocytosis,^{1,2} which results in drug payload exposure to low pH in the lysosomal compartments. The residence time of the vehicle and the drug inside lysosomes can be measured, in principle, if a pH sensor is incorporated into the formulation. pH-sensitive fluorochromes have been used to ascertain the pH of cellular compartments.^{3–5} A protein or other macromolecule is labeled with a pH-sensitive probe, and the fluorescence emission is monitored as it passes into and moves through the cell.^{3–5} Several fluorochromes are reported to have pH sensitivity,⁶ including BCECF, BCPCF, SNARF, cyanines, and fluorescein.^{5–8} Specifically, the pH-sensitive cyanine derivative, CypHer5, developed by Mujumdar and Smith^{9–11} and characterized by Briggs and Cooper,^{3,4} has been used as a pH sensor of lysosomal compartments. The pK_a varies among CypHer5 analogs and ranges from 6.1 to 7.5. CypHer5 analogs also have the advantage of longer excitation and emission

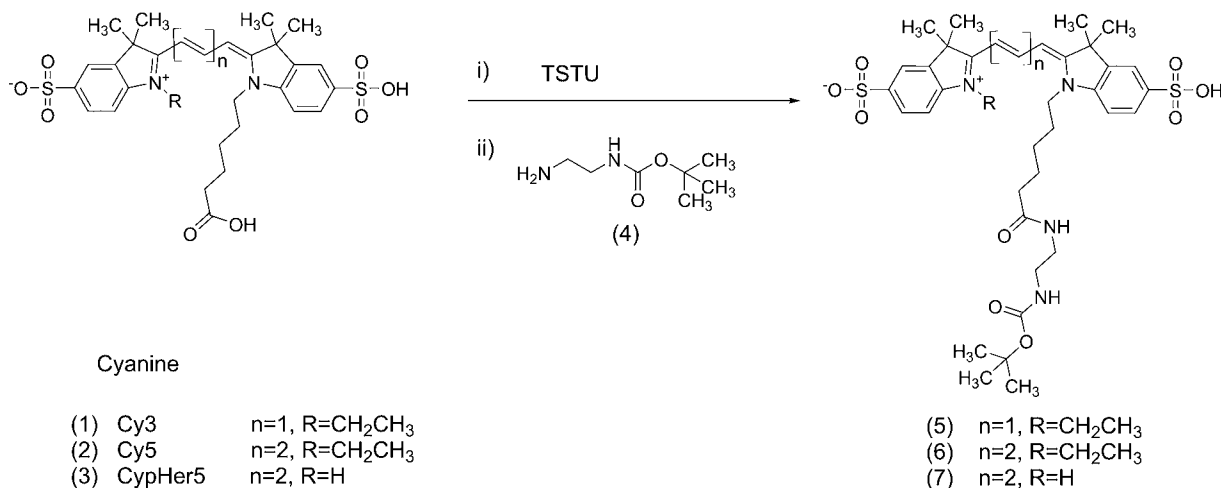
wavelengths ($\sim 645/665$ nm ex/em),^{3,4} compared with fluorescein (494/518 nm ex/em);¹² thus, detection is less likely to be confounded by cellular autofluorescence. Most recently, a CypHer5-based probe was developed by Grover et al. to measure pH variations in β_2 -adrenergic receptor trafficking and to study surface-to-endosome intracellular transfer processes in dendritic cells.¹³

In this study, we have devised novel synthesis strategies to incorporate pH-sensitive cyanine fluorochromes into perfluorocarbon (PFC) nanoemulsion reagents. As described herein, PFC nanoemulsions have received recent significant interest as ¹⁹F MRI imaging agents for clinically relevant *in vivo* cell tracking^{14–18} and as theranostic vehicles.^{19,20} Here, we conjugate CypHer5 to a linear perfluoropolyether (PFPE) PFC molecule prior to nanoemulsion formulation. Additionally, we have synthesized nanoemulsions containing blended PFPE conjugates in the fluorocarbon phase that have a covalently attached reference fluorophore with a different emission

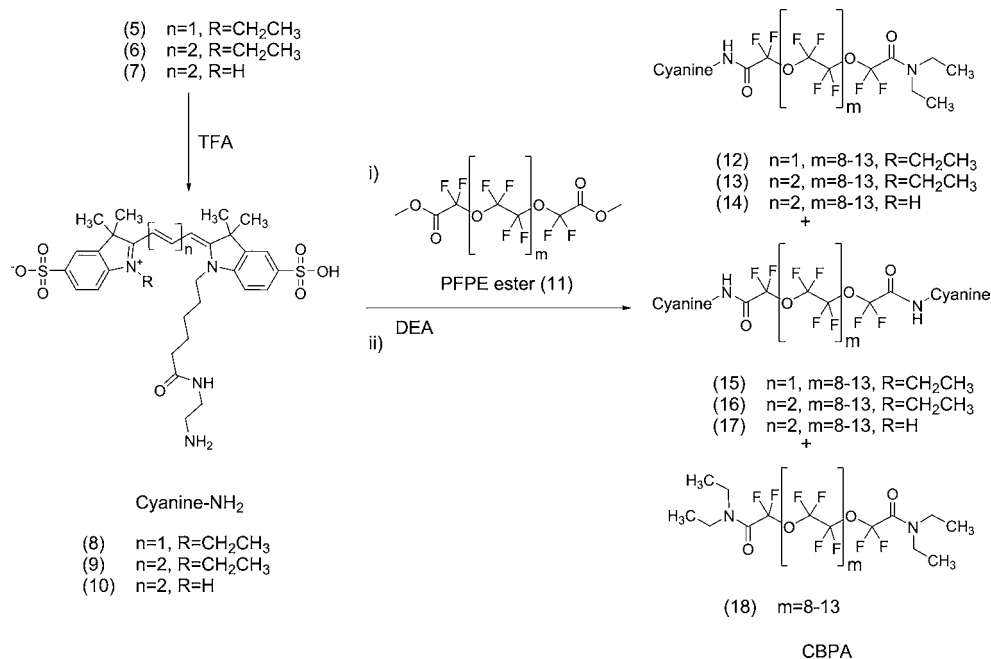
Received: July 23, 2013

Published: October 30, 2013

Scheme 1. Synthetic Scheme of Cyanine-NBoc Conjugates



Scheme 2. Synthesis of CBPAs. Each CBPA is a mixture of PFPE derivatives where cyanine is Cy3, Cy5, or CypHer5 fluorogen and composition of each CBPA is: Cy3-PFPE-oil (12, 15, and 18), Cy5-PFPE-oil (13, 16, and 18) and CypHer5-PFPE-oil (14, 17, and 18)



wavelength maximum (Cy3) that is insensitive to the pH environment of the nanoemulsion. This feature allows ratiometric measurement of absolute microenvironment pH from a reference calibration curve. These new nanoemulsion 'biosensors' can be used to assay intracellular pH in proximity to the nanoemulsion droplets in living cells using flow cytometry and fluorescence microscopy. Development of a fluorescent pH-sensing fluorocarbon nanoemulsion permits tracking of the probe in the cell and reports on the pH of the environment of the ¹⁹F probe. Additionally, our probes can track intracellular localization and can potentially be used to target site-specific organelles; importantly, they are durable, self-delivering, and bright. Our method of design (pH sensor conjugated to PFC) prevents separation of the pH sensor from the fluorocarbon, which is essential to reporting the pH of the fluorous phase location within the cell.

Formulation of stable and effective pH-sensing nanoemulsions offers unique challenges. The fluorogenic portions of the PFPE-biosensor conjugate must retain chemical and photo stability during synthesis. Moreover, although CyDyes in general have been useful as fluorescent labels for proteins and antibodies, it was not clear that they would retain their spectral properties once formulated into nanoemulsions by high-shear microfluidization. Importantly, the final product must be nontoxic to cells, readily taken-up by cells upon coincubation, and retain sensor function within the intracellular milieu. We briefly describe the process we have developed to optimize the dye-PFPE conjugation, nanoemulsion formulation, cell labeling, and fluorescence (pH) quantification. We demonstrate that the CypHer5-PFPE labeled nanoemulsion retains its sensitivity to pH following nanoemulsion formulation. Flow cytometry and ratiometric fluorescence were used to generate a calibration curve and show that the pH of the cellular compartment of 9L

glioma cells that contain the internalized nanoemulsion changes to approximately pH 5.5 over a 3 h period following labeling. Complete details of the methods used are described in Supporting Information.

2. RESULTS

2.1. Synthesis and Formulation of Nanoemulsions.

2.1.1. Synthesis of Cyanine-PFPEs. Linear PFPE was directly conjugated to fluorescent probes by expanding the methodologies of Janjic et al.^{21,22} Starting from preparative high-performance liquid chromatography (HPLC)-purified carboxylic acids of fluorescent dyes,^{3,4,23} free acids were converted to *N*-hydroxysuccinimidyl esters (NHS-esters) using *N,N,N',N'*-tetramethyl-*O*-(*N*-succinimidyl)uronium tetrafluoroborate (TSTU) and then conjugated via amine groups to *tert*-butyl carbamate (Boc)-protected diamine derivatives according to Scheme 1. Dye-free acids (CypHer5, Cy3.29 or Cy5.29, **3**, **1** and **2** respectively) were derivatized to make NBoc conjugates (**5**, **6**, **7**) using ethylenediamine-NBoc in organic solvents and purified by preparative HPLC. The Boc-protected dye was purified by reversed phase HPLC, deprotected with trifluoroacetic acid (TFA), and conjugated to the highly reactive PFPE ester as described elsewhere²¹ and as shown in Scheme 2. When Cy3-PFPE and CypHer5-PFPE were both included in the ratiometric nanoemulsion formulations, 3 M hydrochloric acid was used instead of 1% TFA to improve Boc-group deprotecting efficiency, which was >98% pure by analytical HPLC. This was performed to ensure that during development of pH calibration curves and cell pH measurements, fluorescent signals from unconjugated precursors were eliminated.

PFPEs are highly hydrophobic and lipophobic, with limited solubility in common organic solvents, but are soluble in fluorinated solvents such as trifluorotoluene, trifluoroethanol, and perfluorohexanes. The NBoc moiety was removed with trifluoroacetic acid, and cyanine-amine conjugates (**8**, **9**, or **10**) were mixed with ethanol and triethylamine, and reacted with PFPE-methyl ester (**11**). More specifically, Cy3.29, Cy5.29, and CypHer5 (**8**–**10**) were coupled at 1% mol ratio of PFPE ester, yielding cyanine blended PFPE-amides (CBPAs). CBPAs are a mixture of mono- and bis-conjugated oils (**12**–**14** and **15**–**17**, respectively) or bis-amide PFPE (**18**) and were used without further separation. Cy3.29-PFPE-oil is a mixture of products **12**, **15**, and **18**; Cy5.29-PFPE-oil is compounds **13**, **16**, and **18**, and CypHer5-PFPE-oil is **14**, **17**, and **18** (Scheme 2).

It has been well documented that the longer the polymethine bridge of a cyanine dye, the less stable the fluorophore.⁶ Because of the environmental sensitivities of the CypHer5 fluorophore, such as chemical reactivity or susceptibility to decomposition, care was taken to preserve the compound stability during synthesis and purification by HPLC (see Supporting Information for details). For optimal stability while in solution, CypHer5 derivatives were kept cold (4 °C) and acidic; however, for long-term storage, cold (–20 °C), solid, and dry conditions were used.

2.1.2. Blending of Cyanine-PFPEs. To make single-dye nanoemulsions (**20**–**22**), CBPAs (**12**–**15**–**18**, **13**–**16**–**18**, or **14**–**17**–**18**) were mixed with PFPE-oxide²¹ (at 5% v/v) with the aid of an equal volume of absolute ethanol. Likewise, PFPE-amide (**19**) was used in place of CBPAs to make a nonfluorescent nanoemulsion control (**23**). To make two-dye, ratiometric nanoemulsions (**24**–**27**), CypHer5-PFPE (nominally **14**), and Cy3-PFPE oils (nominally **12**) were blended in molar stoichiometries using an equal volume of

absolute ethanol. Single component ratiometric controls (**28**–**29**), containing only one dye, were made by blending PFPE-amide (**19**) with either **12** or **14**. The ratiometric contribution of each dye was determined by fluorescence synchronous excitation/emission (ex/em) scans in pH 5.8 phosphate buffer^{3,4} using methods described in Supporting Information, resulting in fluorescence ratios of the oils ranging from 1 to 10 times CypHer5 to Cy3 signal. Likewise, ratiometric PFPE-conjugates were mixed with PFPE-oxide²¹ (at 4.9% v/v) with the aid of an equal volume of absolute ethanol.

Blended PFPE conjugate oils behave as a stable and uniform fluoruous phase.^{21,24} The ratio of the CBPA to PFPE-oxide was 1:100; the fluorescent signals would be too saturated if CBPAs were used at full concentration for the nanoemulsion and would cause dye quenching and loss of signal.

Several formulations of CypHer5-PFPE to Cy3-PFPE were blended in various stoichiometries (Table 1). CypHer5-PFPE

Table 1. Listing of nanoemulsion formulation products and PFPE–conjugate composition. Ratio value (CypHer5:Cy3) is post-formulation

product	nanoemulsion name	nominal reagent components (ratios)
20	Cy3-PFPE	12
21	Cy5-PFPE	13
22	CypHer5-PFPE	14
23	PFPE-amide	19
24	ratiometric CypHer5-PFPE: Cy3-PFPE (0.6:1)	14:12 (0.6:1)
25	ratiometric CypHer5-PFPE: Cy3-PFPE (1:1)	14:12 (1:1)
26	ratiometric CypHer5-PFPE: Cy3-PFPE (5:1)	14:12 (5:1)
27	ratiometric CypHer5-PFPE: Cy3-PFPE (8:1)	14:12 (8:1)
28	single component ratiometric control CypHer5-PFPE: PFPE-amide (1:1)	14:19 (1:1)
29	single component ratiometric control PFPE-amide: Cy3-PFPE (1:1)	19:12 (1:1)

and Cy3-PFPE were blended in volume ratios of known concentrations for ease of handling; however, the fluorescence stoichiometry reported in the final formulation is by synchronous fluorescence measurement in pH 5.8 phosphate buffer, as described in Section 2.2.1. Initially, ultrasonication was thought to be a good method to blend the CBPA oils prior to emulsification, but CypHer5-PFPE oil (**14**, **17**, and **18**) did not withstand the process. This was most likely due to the localized heating that occurs during ultrasonication.^{25–27} For this reason, high-pressure microfluidization was used to process the nanoemulsions.

2.1.3. Formation of Nanoemulsions. Single dye nanoemulsions containing Cy3-PFPE, Cy5-PFPE, or CypHer5-PFPE and ratiometric nanoemulsions containing mixtures of Cy3-PFPE and CypHer5-PFPE were prepared using the same process. Blended PFPE oils (Section 2.1.2) were mixed with surfactants comprising aqueous Pluronic F68 and polyethyleneimine solutions, while mixing with vortex (see Supporting Information and Table S1 for formulation details), followed by 10–15 cycles through Microfluidizer (M110S, Microfluidics, Inc., Newton, MA). The size of the final nanoemulsions was 150–175 nm, with a polydispersity index (PDI) of ~0.10 (Figure 1), as measured by dynamic light scattering (DLS). Nanoemulsions remained stable for over 12 months (Figure

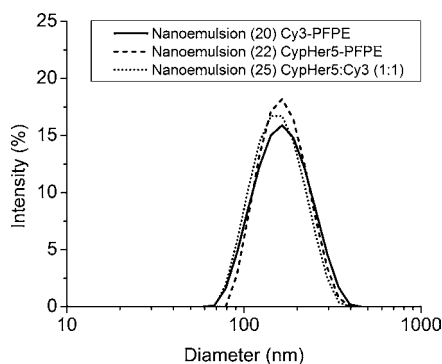


Figure 1. Size distribution by intensity of nanoemulsions 20, 22, and 25.

S16). Further details and discussion of synthesis and formulation are presented in Supporting Information.

2.2. Characterization of Nanoemulsions. **2.2.1. pH-Sensitivity and Spectral Properties of Nanoemulsions.** The absorption and emission (em) spectra of a CypHer5-PFPE nanoemulsion (22), without Cy3-PFPE, are shown in Figure 2, along with spectrally similar and pH-insensitive Cy5-PFPE nanoemulsion (21) for comparison. Absorbance spectra could not be obtained from the conjugated dyes at low molar ratios in the nanoemulsion due to interference from components of the formulation; therefore, excitation (ex) spectra were obtained instead (Supporting Information and Figure S17, panels E,F). However, absorbance spectra could be directly obtained using the PFPE-conjugates (12–14) solvated with ethanol (Figure 2A). The absorption spectrum of CypHer5-PFPE (14) changes with pH, and the longer wavelength band dominates at low pH.

The emission signal with excitation at 630 nm increases at low pH as expected (Figure 2C). As was demonstrated by Briggs and Cooper,^{3,4} a plot of the emission signal versus pH allows determination of the pK_a for CypHer5 (Figure S17C). This plot, normalized to the signal at pH 5.8, yields a pK_a of 6.8 for CypHer5 in the nanoemulsion.

The addition of pH-insensitive Cy3-PFPE to formulations 24–27 allowed quantification of nanoemulsion in labeled cells and also ratiometric calibration of pH using both CypHer5 and Cy3 signals (Figures 3 and S18). In these two-dye nanoemulsions, the CypHer5 emission spectra were the same for 24–27 (Figure 3A) and matched the single-dye CypHer5-PFPE nanoemulsion (22), as shown in Figure 2C. However, when greater amounts of CypHer5 are added to the nanoemulsion relative to Cy3, excitation of Cy3 at 530 nm also excites CypHer5 on the blue side of its absorption band (Figure 2A) to give fluorescence at 670 nm. This is more noticeable for nanoemulsion 26, which has a higher content of CypHer5 than 24 (Figure 3B). Because of this complication, quantification of the relative Cy3 and CypHer5 compositions of ratiometric nanoemulsions (24–27) was performed with synchronous fluorescence scans. Simultaneously scanning both excitation and detection wavelengths with a 20 nm wavelength separation (the Stoke's shift of both fluorophores) enabled measurement of each signal without spectral spillover. Using fixed wavelength excitation requires two emission scans and results in two broad-band emission spectra, one corresponding to each chromophore (as in Figure 3A,B); in contrast, the variable excitation wavelengths of a synchronous fluorescence scan produce a single spectrum that contains two narrow-band peaks, corresponding to the maximum excitation of each chromophore (as in Figure 4). Cy3 excites maximally at

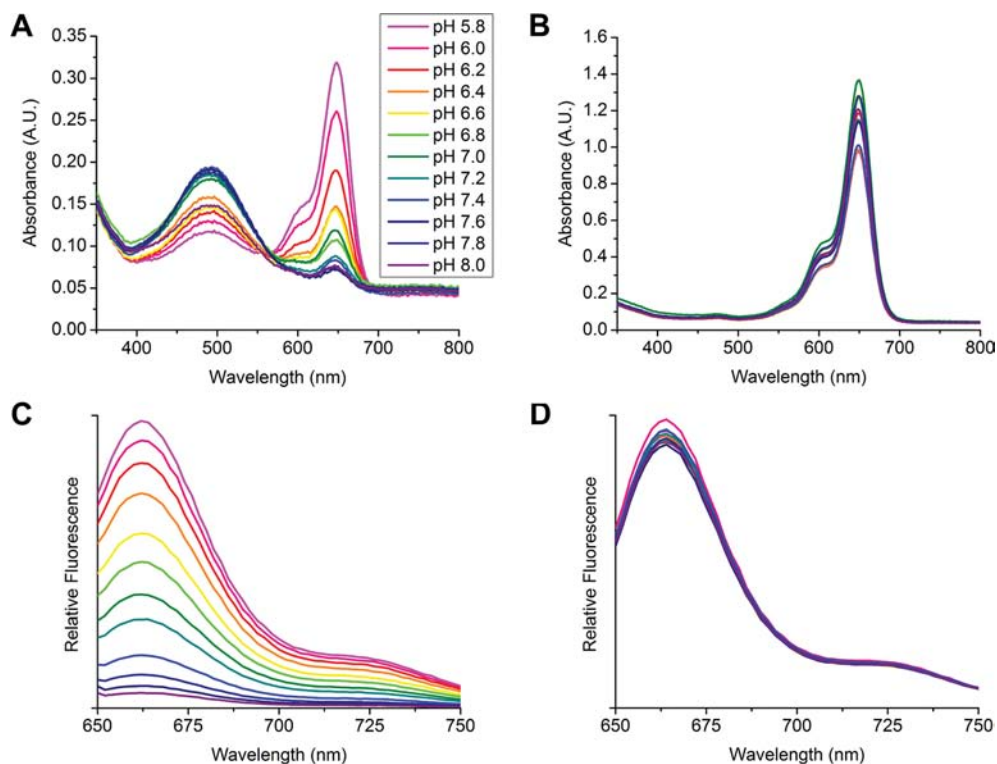


Figure 2. Spectral properties of cyanine-PFPE conjugates in phosphate buffers. Inset (A) shows pH range for series. Absorbance spectra (A) of CypHer5-PFPE oil (14, 17, and 18) and (B) Cy5-PFPE oil (13, 16, and 18). Fluorescence emission spectra of CypHer5-PFPE (C) and Cy5-PFPE (D) nanoemulsions 22 and 21, respectively. Excitation wavelength was 630 nm.

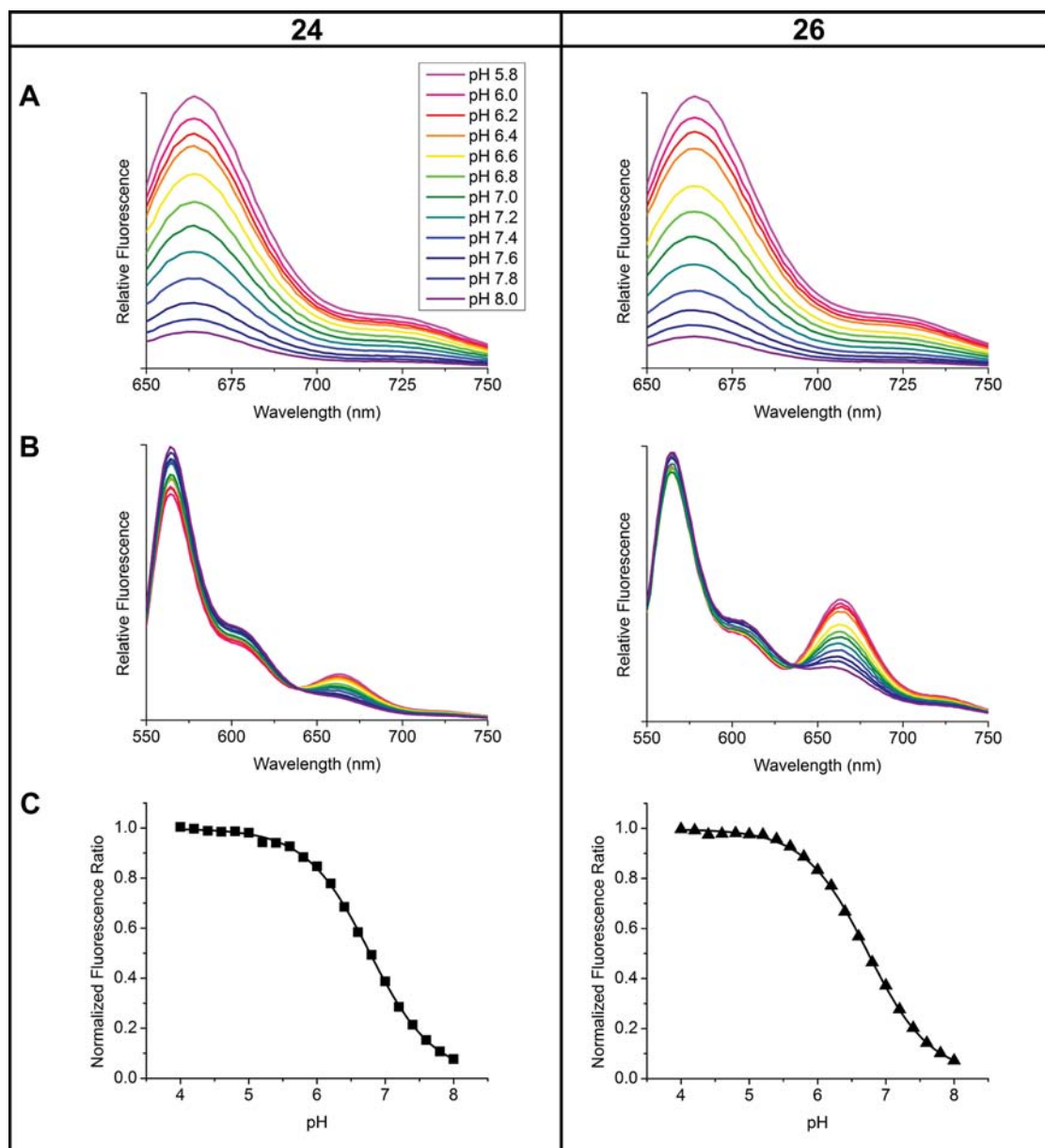


Figure 3. Fluorescence spectra and pH response of ratiometric nanoemulsions **24** and **26** in phosphate buffers. Inset (A) shows pH range for series. Emission scans ex 630 nm (A) and em 530 nm (B). pH-ratio calibration curves (C) normalized to maximum fluorescence ratio value (at pH 4.0), averaged from synchronous and fixed wavelength scanning methods. pK_a of both formulations is 6.8.

544 nm, has an emission peak at 564 nm (Figure 3B), and produces a pH-insensitive synchronous scan peak at 548 nm (Figure 4). CypHer5, on the other hand, has a pH-sensitive maximal absorption at 644 nm and emission at 664 nm (Figure 3A) with a pH-sensitive synchronous scan peak at 649 nm (Figure 4). In the synchronous fluorescence spectra, the intensity of each peak corresponds to the relative abundance of each chromophore and thus allows formulation stoichiometries to be compared. Nanoemulsions **28** and **29** contain only one peak because these are single component ratiometric controls. Ratiometric measurements using fixed wavelength and synchronous scanning modes are discussed further in the Supporting Information.

These fluorescence scanning methods enabled the measurement of pK_a of 6.8 for the CypHer5 fluorophore in the nanoemulsions (Figure 3C). The pK_a curve profiles (normalized to 1.0 at pH 4.0) were identical for two-dye nanoemulsions

(**24**–**27**), regardless of ratiometric stoichiometry (Figure S20). A pK_a value of 6.8 is comparable to the values of the CypHer5 dye in aqueous buffers obtained by our lab and others.^{3,4} In addition, similar plots for CypHer5-NBoc (**7**) and PFPE nanoemulsions at different dye concentrations (nanoemulsions **24**–**27**) in buffers yield the same pK_a . This is interesting in view of possible localization distributions the CypHer5 molecule might occupy within nanoemulsion droplets. The result indicates that the CypHer5 fluorophores, which carry two sulfonic acid groups, lie at the surface of the nanoparticles exposed to the local polar environment. It is probable that the CypHer5 fluorophores that are covalently bound to the PFPE molecules are thus amphipathic (as in a large micelle) and associate with nonpolar unlabeled PFPE molecules that form the core of the nanoemulsion droplet.

The quantum efficiencies of the fluorescent nanoemulsions could not be measured directly because light scatter from the

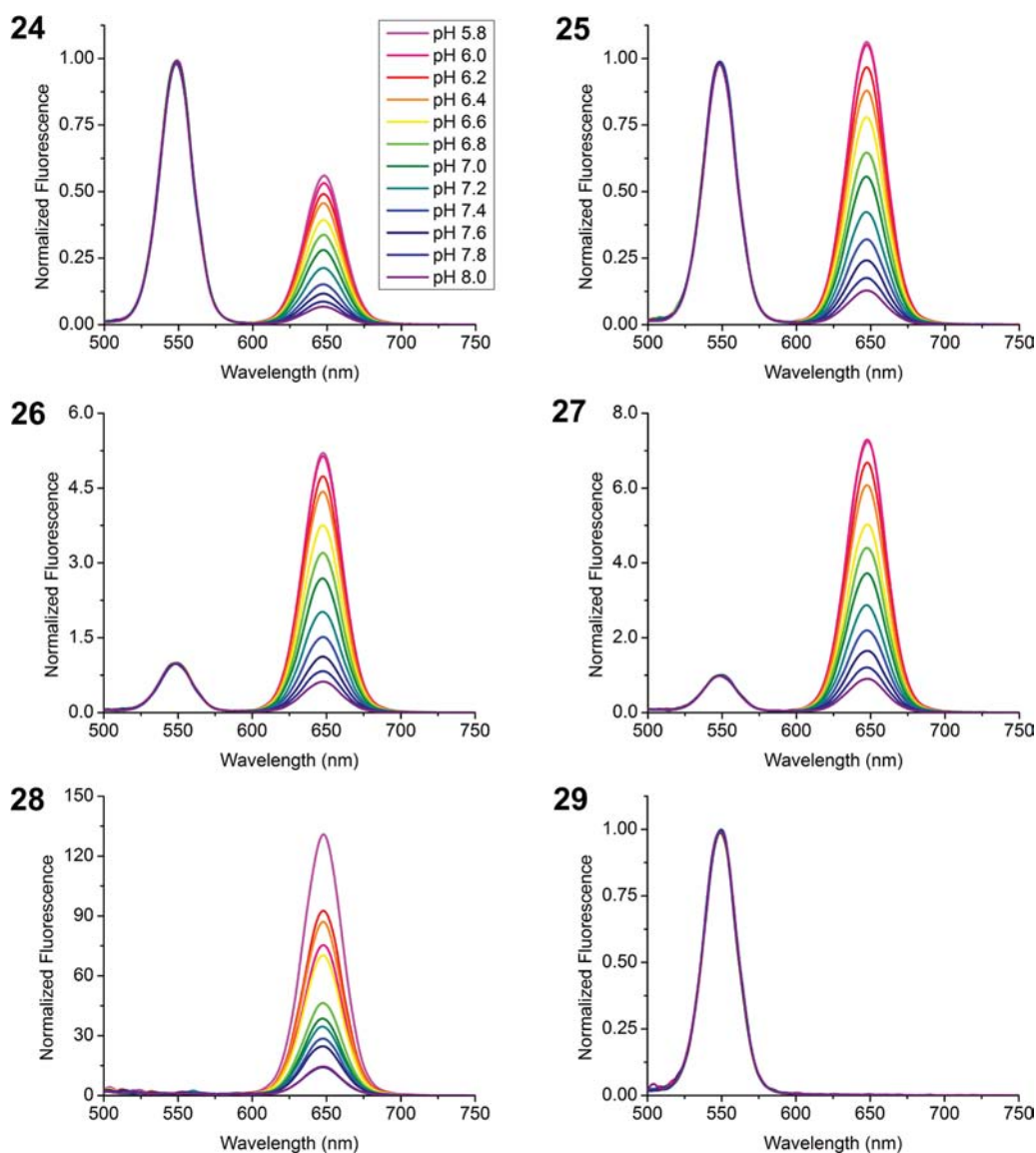


Figure 4. Synchronous scans (20 nm offset) of ratiometric nanoemulsion formulations 24–29 in phosphate buffers. Inset (24) shows pH range for series. Single component ratiometric control nanoemulsion 28 contains no Cy3-PFPE; 29 contains no CypHer5-PFPE. All spectra are normalized to ex 548 nm (Cy3).

colloidal dispersion is very intense. However, the quantum efficiencies of fluorophores Cy3 and CypHer5 have been addressed previously by Mujumdar, Briggs, and Cooper.^{3,4,23} The values are likely to be unchanged with side-chain modification. Since the spectra of the nanoemulsions are comparable to those of the parent dyes, it is expected that the quantum efficiencies of the nanoemulsions will likewise be comparable to the parent dyes.

Optimization of the stoichiometry of CypHer5 relative to Cy3 is essential in developing ratiometric reagents that are suitable for platforms such as flow cytometry or fluorescence microscopy; a ‘one size fits all approach’ may not be best. We have observed that certain formulation stoichiometries are better than others when used for spectral studies in cells and for loading cells to be used during *in vivo* studies; it is essential to have a strong Cy3 signal so that the autofluorescence of the cells does not dominate quantification of the reference signal (discussed further in Sections 2.3.2 and 2.3.3). The synchronous scan method provides an easy way to determine

the amount of CypHer5-PFPE that should be added to the formulation so that the CypHer5 to Cy3 signal ratios are in an optimal range of 0.5–10, as displayed in Figure 4. However, preformulation measurement of blended CypHer5 and Cy3 PFPE-conjugate stoichiometries by synchronous scan did not equal postformulation measurements, where CypHer5 content was consistently 40% lower. We speculate that this apparent dye loss is due to its decomposition of this sensitive fluorophore during processing. Preformulation quantities of CypHer5-PFPE were adjusted to anticipate dye loss during processing (see Supporting Information).

2.2.2. Role of Energy Transfer. Förster resonance energy transfer (FRET) can occur when a pair of fluorophores has overlapping excitation and emission spectra, and the molecules are within close proximity. The emission of the shorter wavelength fluorophore (donor) nonradiatively transfers its excitation energy to the longer wavelength fluorophore (acceptor), inducing fluorescence emission from the acceptor.²⁸ Cy3 and Cy5 are a well-known energy transfer pair used for

FRET measurements in biophysical studies. For this pair, energy transfer can be observed when the donor and acceptor are within 8 nm.²⁹ Since CypHer5 and Cy3 are spectrally similar when CypHer5 is protonated, there is potential for FRET due to the Cy3-CypHer5 pairing. Efficient energy transfer could potentially complicate pH calibrations and estimation of the localized cellular pH of internalized nanoemulsions. We observed no evidence of energy transfer when Cy3 and CypHer5 were formulated in separate nanoemulsions (29) and (28), and then mixed. This is not surprising, as it is expected the average spacing of the two fluorophores would not be close enough in mixed, but separately formulated nanoemulsion droplets. However, if the fluorophores are formulated within the same nanoemulsion droplet, as in nanoemulsions 24–27, dye concentrations may be sufficient to bring the fluorophores within FRET proximity. Additionally, if FRET were to occur in our nanoemulsions, it would be more probable when Cy3 and CypHer5 molecules are present in equal quantities within the same nanoemulsion droplet.

To investigate FRET, we used the nanoemulsion containing the highest concentrations of Cy3 and CypHer5 (25). Because of the spectral overlap of Cy3 and CypHer5, and hence their energy transfer, depends on pH, nanoemulsion samples were diluted into hydrochloric acid (50 mM) to ensure complete protonation of CypHer5. The concentration of single-dye control nanoemulsions (28 and 29) was adjusted to equal the corresponding Cy3 or CypHer5 component of 1:1 ratiometric nanoemulsion (25) using the emission maxima of Cy3 and CypHer5 wavelengths accordingly (564 and 662 nm), with excitation at 530 and 630 nm. The dyes were scanned separately, and thus broad excitation or potential energy transfer was excluded from concentration determinations. Initially, the spectral properties of each dye were determined individually using the single-dye controls. A nanoemulsion containing only Cy3 (29) was excited at the Cy3 excitation wavelength (530 nm), and the emission of Cy3 was measured at the CypHer5 emission wavelength (662 nm). This determined the amount of Cy3 emission spillover that could mimic energy transfer. This spillover was 5% of the Cy3 emission maximum at 564 nm. Similarly, a nanoemulsion containing only CypHer5 (28) was excited at the Cy3 excitation wavelength and the emission of CypHer5 was quantified; the result was 18% of the CypHer5 emission maximum at 662 nm, which indicates the efficiency of CypHer5 excitation at 530 nm. Finally, the same measurement done for Cy3 alone (29) was repeated using a nanoemulsion containing both Cy3 and CypHer5 (25), and the emission due to 530 nm excitation comprised 33% of the CypHer5 emission maximum at 662 nm. Additionally, for all nanoemulsions (25, 28, 29), the direct emission intensities of Cy3 and CypHer5 (564 and 662 nm) were measured with excitation at 530 and 630 nm. The instrument settings for all three nanoemulsions were identical. Energy transfer was then estimated by deconstructing the total emission intensity at 662 nm for nanoemulsion 25, using information gained from these measurements. We observed 41% of the intensity of 25 was due to Cy3 emission signal that spills over into the CypHer5 fluorescence channel (based on percentage measured using 29), 54% of the signal intensity was due to excitation of CypHer5 by 530 nm excitation (based on percentage using 28), and the remaining 5% of the emission intensity was attributed to energy transfer. With an estimated 5% efficiency, it is unlikely that energy transfer is a significant

interfering factor in our ratiometric nanoemulsion fluorescence studies.

2.2.3. Fluorescence Stability of Bulk Ratiometric Nanoemulsions. The fluorescence stability of bulk ratiometric nanoemulsions (24–29) was characterized at 4 and 37 °C. Nanoemulsion samples were taken every 1–2 weeks and diluted (2% v/v) into pH 5.8 phosphate buffer. In fluorescent synchronous scans, nanoemulsion fluorescent signals decreased rapidly (100% of CypHer5 and 75% of Cy3 within 6 weeks) at 37 °C storage, while those kept at 4 °C were much more stable (~60% for CypHer5 and 50% for Cy3 over an extended 60 week period), further described in Supporting Information and shown in Figure S21, top panel. Fluorescent ratios (CypHer5/Cy3) were stable for several months at 4 °C, while at 37 °C, ratios converged to 0 within 6 weeks due to decomposition of CypHer5 (see Figure S21, bottom panel). For formulations with a higher content of CypHer5 (27), fluorescence ratios dropped 50% over 60 weeks, while those with a lower content of CypHer5 (24), dropped only 25%. At 4 °C, both dyes decompose at similar rates; however, the CypHer5 signal dropped significantly relative to Cy3. For these reasons, bulk ratiometric nanoemulsion products should be stored at 4 °C, rather than at ambient or higher temperatures.

2.2.4. Stability of Fluorescence Signals under Cell Labeling Conditions. Cell labeling experiments often subject nanoemulsions to 37 °C, and media containing proteins or biomolecules for many hours, thus the fluorescence stability and pH sensitivity of the reagents in proteinaceous media were evaluated. Ratiometric nanoemulsions 24–26 were diluted into cell culture media [Dubelco's modified Eagle medium, (DMEM), containing 10% fetal bovine serum, 1% penicillin streptomycin, 25 mM 4-(2-hydroxyethyl)-1-piperazineethanesulfonic acid (HEPES) and free of Phenol Red indicator] or a deionized water control at typical cell labeling concentration (1 mg/mL), and then incubated at 4 or 37 °C. Sample stability and pH sensitivity of CypHer5 and Cy3 signals were measured by fixed wavelength scans (ex/em 648/668 nm and ex/em 548/568 nm), followed by subsequent dilution into high potassium HEPES buffers⁵ to fix the sample pH during the measurement (see Supporting Information for detail). Fluorescence signals of CypHer5 and Cy3, and ratios of CypHer5/Cy3 normalized to pH 5.5 value, were plotted; results are shown for nanoemulsion 26 (which contained the highest amount of CypHer5) in Figure S22, panels A–B. When incubated in DMEM, Cy3 signals remained steady throughout 48 h, while CypHer5 decreased by 33% at both 4 and 37 °C. However, when incubated in water at 37 °C, the CypHer5 signal decreased 45% during the same time. The relative preservation of CypHer5 incubation in DMEM compared to water may be attributed to a more shielded environment created by the media components (such as serum proteins) that may make it less susceptible to effects of degradation agents. Despite some loss of CypHer5 fluorescence signal, the pH sensitivity was retained in all samples. Ratiometric pH function across pH 5.5–7.5 was similar for each nanoemulsion/media combination when ratios were normalized to pH 5.5 at the same time point (see Figure S22C). Overall, through using normalized fluorescence ratios, these results show that pH sensitivity of ratiometric nanoemulsions is retained under typical cell labeling conditions.

2.3. Biological Evaluation of Ratiometric Nanoemulsions. Four of the ratiometric nanoemulsions prepared in this study (24–27), were used to label 9L glioma cells, and these cell preparations were then analyzed by three commonly used

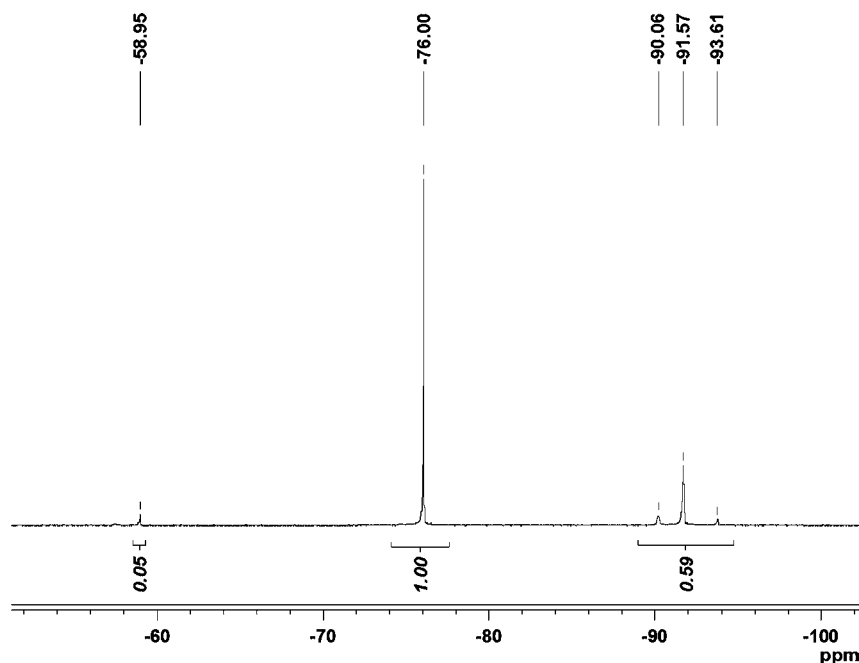


Figure 5. Nanoemulsion uptake by ^{19}F NMR. 9L cells labeled with ratiometric nanoemulsion 26. ^{19}F NMR in 0.1% TFA of 9L cells labeled at 5 mg/mL. Cells were lysed for measurements.

fluorescence detection platforms, including a fluorescent plate reader, fluorescence microscope, and flow cytometer. Optimal CypHer5/Cy3 stoichiometries were determined for each platform.

2.3.1. Nanoemulsion Cellular Uptake by ^{19}F NMR and Fluorescence Detection. Glioma cells (rat 9L) were co-incubated with nanoemulsions 20–27 in media for 3 h at 37 °C, followed by a wash step with phosphate buffered saline (PBS). The average nanoemulsion uptake during the labeling period was determined using ^{19}F NMR of cell pellets to measure the ^{19}F per cell, as described elsewhere.¹⁸ A representative ^{19}F NMR spectrum of a labeled cell pellet is shown in Figure 5. At the optimum labeling doses, defined as 80% viability compared to unlabeled cells, the ^{19}F loading ranged from 0.1 to 1.0×10^{11} ^{19}F /cell (Figure S23).

To correlate ^{19}F NMR signals with the fluorescent signals of CypHer5 and Cy3 in the ratiometric nanoemulsions, 10% (by volume) of cell lysate isolated during dose optimization was read using a plate reader at fixed wavelengths (ex/em 530/564 nm for Cy3 and ex/em 630/664 nm for CypHer5). The amount of nanoemulsion (ng/cell) taken up by the cells was calculated from linear calibration curves of nanoemulsions 22–27 in 0.1% TFA. The number of fluorine atoms per cell is directly proportional to the mass of nanoemulsion per cell. The concentration of bulk nanoemulsion (in mg/mL) is determined before cell labeling by quantifying the number of fluorine atoms using ^{19}F NMR following methods described by Janjic.²¹ Additionally, the direct conjugation of the fluorescent probes to the fluorocarbon ensured direct correlation of fluorescence signals with ^{19}F NMR signal. Excellent agreement between ^{19}F uptake per cell by NMR and CypHer5 and Cy3 uptake per cell measured by fluorescent plate reader was observed when the data were normalized to the highest labeling concentration and unlabeled controls were subtracted as background (Figures 6 and S24). Normalized uptake data varied at the lowest labeling concentration (0.125 mg/mL), where the signal of the fluorescent dyes approached the noise level (these points

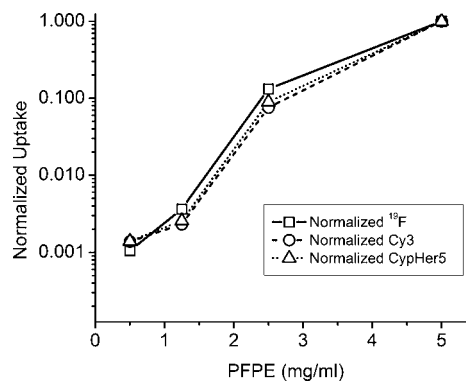


Figure 6. Nanoemulsion uptake by ^{19}F NMR and fluorescence methods. 9L cells labeled with ratiometric nanoemulsion 26. Dose curve by ^{19}F NMR and Cy3 and CypHer5 fluorescence. Cells were lysed for measurements.

were not included on the plots). It should also be noted that since the cells are lysed and the lysate contains 0.1% TFA, CypHer5 is fixed in the protonated form and thus cannot report the pH of the cellular material in this experiment; the experiment only demonstrates correlation between both fluorophore signals and ^{19}F signals of the PFPE-conjugates. These results indicate that all four ratiometric formulations are well suited for fluorescent plate reader experiments, as the ^{19}F content of PFPE-loaded cells can be readily quantified from Cy3 fluorescence. Importantly, simple and low-cost fluorescence plate reader measurements can thus be used to assay the degree of cell labeling for *in vivo* MRI cell tracking applications.^{14,18}

2.3.2. Selection of Ratiometric Formulations for Fluorescence Microscopy. Confocal microscopy was used to image living 9L cells that were labeled at optimal doses with ratiometric nanoemulsions 24–27 (see Supporting Information). Using nonoverlapping emission filters and a spinning disk confocal system, ratios of signals from the CypHer5 and Cy3

channels were measured. Ratiometric nanoemulsion **26** (Figure 7) showed strong signals in the CypHer5 channel (Figure 7A,

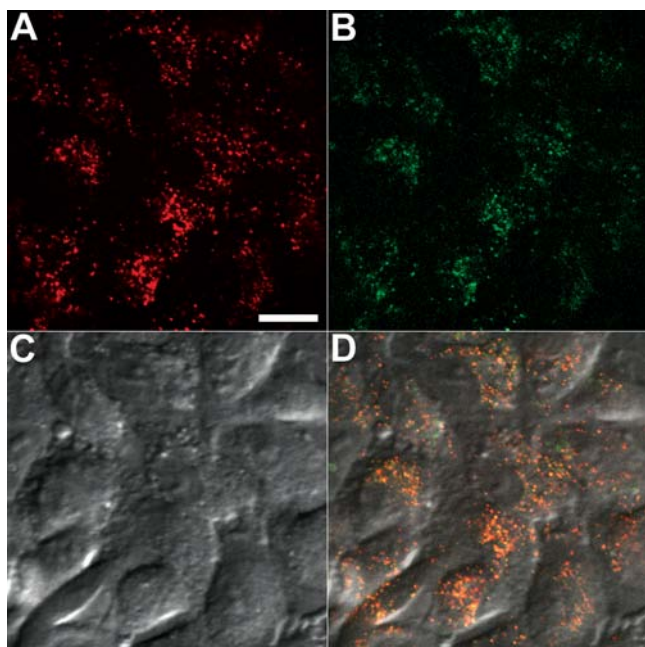


Figure 7. Confocal microscopy images of ratiometric nanoemulsion **26** labeled 9L cells, showing channels: CypHer5 (A), Cy3 (B), DIC (C), and merged channels (D). Scale = 10 μm .

red) and in the Cy3 channel (Figure 7B, green), which were substantially above background noise. The differential interference contrast (DIC) and fluorescence images confirmed that the fluorescent labeling was confined to intracellular regions consistent with an endocytosis uptake mechanism^{1,2} (Figure 7A–C). Also, the CypHer5 and Cy3 signals showed colocalization as expected (Figure 7D, yellow). Formulations with a higher content of CypHer5-PFPE (**26**, **27**) showed brighter fluorescence and thus are better candidates for fluorescence microscopy. The low Cy3 signal in formulation **27** was barely detectable and thus nonoptimal compared to **26**. Preliminary pH calibration experiments in cells indicate that the ratio change is readily observed when there is <3-fold difference between the intensity of CypHer5 signals compared to Cy3 signals (data not shown).

2.3.3. Selection of Ratiometric Formulations for Flow Cytometry. Flow cytometry was also used to detect 9L cells labeled with ratiometric nanoemulsions **24**–**29** (see Section 2.3.1). After labeling, cells were washed, detached and resuspended in PBS for flow cytometry analysis. Cy3 and CypHer5 channel histograms of ratiometric nanoemulsions **24**–**29** were compared to nonfluorescent nanoemulsion **23** as a control (Figures 8, S26–S27). CypHer5 and Cy3 signals were readily differentiated from nonfluorescent nanoemulsion in control nanoemulsions **28** and **29**. However, Cy3 signals were differentiable from nonfluorescent labeled cells only in nanoemulsions that contained equal or greater amounts of Cy3-PFPE compared to CypHer5-PFPE (such as **24** and **25**); while CypHer5 signal was differentiable from nonfluorescently labeled cells in all four formulations (**24**–**27**) evaluated. For this reason, nanoemulsion **24** was optimal for flow cytometry. Single-dye nanoemulsions (**20**–**22**) were also evaluated using flow cytometry and exhibited fluorescent population distribu-

tions similar to the corresponding single component control nanoemulsions (**28**, **29**), with Cy3-PFPE (**21**) being similar to CypHer5-PFPE (**22**). When ratios of the mean fluorescence histograms were calculated (mean 685 nm/mean 575 nm), the ratios increased as the content of CypHer5 was increased in the formulation stoichiometry (Figure 9).

2.4. Intracellular pH Measurement. 2.4.1. Generation of Intracellular pH Calibration Curve. Ratiometric nanoemulsions were used to measure the intracellular pH in live cells using flow cytometry. When a fluorophore is monitored at its pH-sensitive wavelength, the magnitude of the signal depends on the amount of probe present as well as the pH. Thus, ratiometric detection methods are employed that use a (pH-insensitive) reference signal at a separate wavelength to provide a measure of the amount of probe present. CypHer5 alone can also be used for pH measurements,^{3,4} but we found that this approach is challenged by a significant amount of cellular autofluorescence at shorter excitation wavelengths or a low absorption coefficient at the isosbestic point. Thus, we formulated nanoemulsions to include a separate pH-insensitive probe in the sample (Cy3) that absorbs and emits at a separate wavelength from the pH-sensitive probe. Also, the relative proportions of Cy3 and CypHer5 in the nanoemulsion can be tuned to provide an optimal detection system (see Section 2.3).

To calculate pH from fluorescence ratios in cells, a ratio-pH calibration curve was initially generated, similar to Figure 3C. Additionally, the cellular environment autofluorescence and scatter impact the calibration and must be taken into account. We employed methods described by Barriere et al.⁵ to obtain the ratiometric calibration in cells. In brief, the calibration curve is obtained by setting the pH of all intracellular compartments to the chosen buffer pH by adding the hydrogen ionophores nigericin and monensin to cells 5–30 min before the flow cytometry measurements.

During nanoemulsion uptake in 9L cells using the above incubation conditions, the Cy3 reference signal was used to quantify the extent of CypHer5 (and ¹⁹F) incorporated during cell labeling. Fluorescence ratios between reporter and reference signals were calibrated intracellularly to external high K⁺ phosphate buffers ranging from pH 5–8 using the pH clamp reagents nigericin and monensin. Mean fluorescence ratios 685/575 nm were calculated, normalized to the pH 5.0 value, and plotted against pH (Figure 10A). Data using the pH clamp reagents showed small increases in side scatter as pH became more acidic, which is indicative of cell swelling and increased granularity. Minimal changes in viability and cell swelling were observed at pH 5–8 during this treatment.

Cellular background autofluorescence was accounted for in the calibration curves. Control cells labeled with nonfluorescent nanoemulsion were treated in the same way using the pH clamp methods. The mean fluorescence values of cells labeled with nonfluorescent nanoemulsion **23** were subtracted from the corresponding histograms, and the 685 nm/575 nm ratios were recalculated and normalized to the maximum pH value (5.0) and plotted against pH. These data were fit to Boltzmann sigmoidal curves. Cellular autofluorescence was a significant contributor to the Cy3 signal and altered the shape of fluorescence ratio–pH calibration curves, as seen by the higher ratio value at pH 8 relative to that of free nanoemulsion (Figure 10A). Background subtraction of nonfluorescent-labeled controls shifted the ratio at pH 8 from 0.36 to 0.11, bringing it closer to the ratio of free nanoemulsion (0.07), indicating

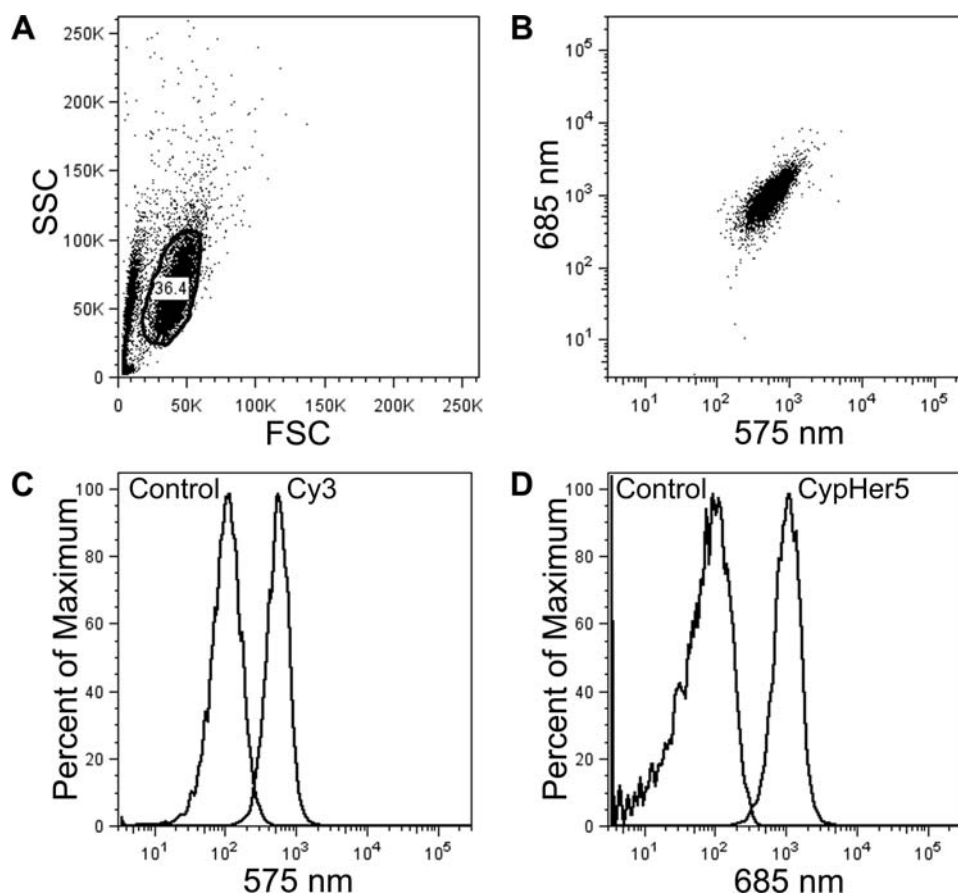


Figure 8. Flow cytometry of 9L cells labeled with ratiometric nanoemulsions. Representative FSC/SSC plot (A) and dot plot (B) for formulation 24; gated region marked by black line (A). Histograms are of live gated cells at (C) 575 nm for Cy3 and (D) 685 nm for CypHer5 and are overlaid control cells labeled with nonfluorescent nanoemulsion 23.

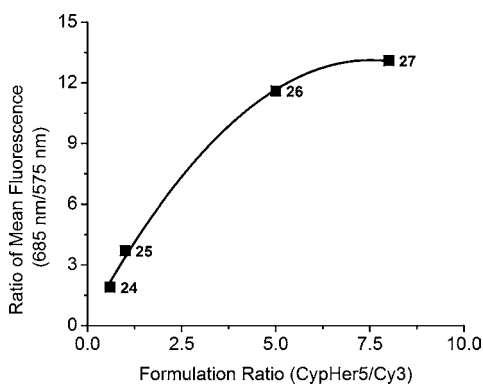


Figure 9. Comparison of ratiometric nanoemulsion formulations by flow cytometry. A plot of mean fluorescence ratio (685 nm/575 nm) against formulation ratio of nanoemulsions 24–27 using 9L cells labeled with ratiometric nanoemulsions. Data points are identified by formulation number.

that intracellular autofluorescence interference could be corrected when subtracted from ratiometric measurements.

2.4.2. Calculation of pH during Nanoemulsion Uptake. Using the calibration curve constructed in Section 2.4.1, we measured the intracellular pH during uptake of nanoemulsion by 9L cells. Measurements were made using ratiometric nanoemulsion 24 at 30 min intervals for up to 3 h. The flow cytometry measurements were made with cells suspended in PBS without ionophores. The Cy3 fluorescence reference signal

(575 nm) was used to quantify the extent of ^{19}F (nanoemulsion) incorporated during cell labeling, which increased 55% over the course of 0.5–3 h. Likewise, the 685 nm CypHer5 signal increased 149% over the same period, indicating both uptake and increased acidity (Figure S30). Fluorescence ratios were calculated from histograms of gated cells, and the pH was determined from the calibration curve that was corrected for autofluorescence (see Supporting Information for details). Results for both corrected and uncorrected data are shown in Figure 10B. The intracellular pH changed from ~ 6.7 to ~ 5.5 from 0.5 to 3 h; the same result was obtained regardless of whether raw or corrected data was used. The intracellular pH progressed to the terminal value of ~ 5.5 at the end of the 3 h, suggesting nanoemulsion trafficking from neutral cytosomes to acidic lysosomal compartments over this time period. However, from the current data alone, it is unknown if the ultimate nanoemulsion fate is the lysosome or if it is recycled back to the cytosomes. Further study using our ratiometric reagent to measure subcellular pH and with confirmation using pharmacological agents is needed.

2.4.3. Experimental Parameters of pH Measurement. To obtain reliable intracellular pH measurements, the same cell preparation must be used to develop the calibration curve and to do the cell measurement, and both should be performed within a few hours of each other. Experimental data must be normalized by the same value used to normalize the calibration curve. Furthermore, it is important that cellular ratio and pH calibration be performed with the same detection instrument

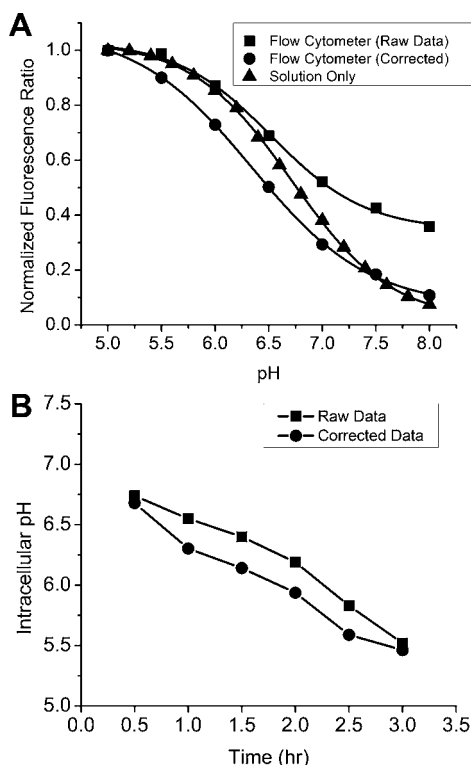


Figure 10. (A) Comparison of pH-ratio curves of pH-clamped 9L cells labeled with ratiometric nanoemulsion 24, free nanoemulsion and autofluorescence correction. (B) Intracellular pH during nanoemulsion uptake showing raw and corrected data.

used for the cell measurements. For example, plate readers, spectrofluorometers, flow cytometers, and imaging microscopes usually have different excitation sources (wavelengths and intensities), different emission monochromators or interference filters with different bandwidths, and different sensitivities for detector sensitivity versus wavelength. For this reason, we used an approach that is solely based on flow cytometry to obtain cellular pH. With this approach, the flow cytometer settings (filter sets, photomultiplier tube voltages, signal amplification) are not changed between calibration and cellular measurements. A calibration curve is needed for each fluorescence platform used during pH measurements.

3. DISCUSSION AND CONCLUSIONS

3.1. Ratiometric Reagent Development. We describe a novel design for PFC-based nanoemulsion reagents with intracellular biosensing properties. A fluorescent pH sensor was directly conjugated to PFPE molecules and formulated into stable and nontoxic nanoemulsions. Four pH-sensitive ratiometric formulations (24–27) of differing CypHer5: Cy3 stoichiometries were optimized for use with fluorescent plate reader, flow cytometer, and fluorescence microscopy platforms. All four ratiometric formulations were suitable for ^{19}F NMR and fluorescent plate reader applications. Quantification of ^{19}F NMR and fluorescence of both dye signals agreed in lysed cells. Nanoemulsion 24 (0.6:1 CypHer5: Cy3) was best suited for flow cytometry, while nanoemulsion 26 (5:1 CypHer5: Cy3) was best suited for fluorescence microscopy. In both of these platforms, the key requirement is to get strong CypHer5 reporter signals to monitor pH changes with as much fluorescence response as possible over the pH range, while

maintaining good discrimination of the Cy3 reference signal over background. Using this reagent stoichiometry optimization approach, further modifications can be made to the reporter or reference fluorophore as additional application requirements emerge.

3.2. Intracellular pH Measurement and Future Applications. Ratiometric reagents were used to determine the intracellular pH of 9L cells during nanoemulsion uptake using flow cytometry. The Cy3 reference signal was used to quantify the degree of nanoemulsion uptake during cell labeling. Cellular autofluorescence was a contributor to the Cy3 signal, and a simple autofluorescence subtraction method was used to improve the accuracy of the calibration curve. The pH changed from ~ 6.7 to ~ 5.5 throughout the progression of the 3 h uptake experiment, indicating nanoemulsion migration to a more acidic environment over the labeling time. PFC nanoemulsion uptake has been studied extensively by Wickline² using nonphagocytic 2F-2B cells. Janjic et al.²¹ suggested that polyamine-driven nanoemulsion uptake is likely driving the labeling in nonphagocytic cells. In the current study, using nonphagocytic 9L cells, labeling studies suggest polyamine-driven uptake mechanism, which was previously identified by Godbey to be an endocytosis mechanism.¹ Therefore, our PFC-probe most likely reports the pH of endosomes.

Intracellular pH measurements have utility in the development of intracellular drug delivery systems and *in vitro* pharmacology studies. PFC nanoemulsions are increasingly being used for *in vivo* cell imaging studies^{14–16,18,30} and as theranostic vehicles.^{19,20,31–33} A particularly compelling application of the pH-sensing technology described herein is to accelerate the development of emerging MRI-based cell tracking technologies,^{14,17,18,21,34–40} one such technology of clinical interest is called ‘*in vivo* cytometry’. In this platform technology, cell populations of interest (e.g., therapeutic cells such as stem cells destined for a patient) are labeled, tracked, and quantified *in vivo*.¹⁴ Cells are initially labeled in culture using PFC nanoemulsions.^{14,21} Following transfer to the subject, cells are tracked *in vivo* using ^{19}F MRI. The fluorine inside the cells yields cell-specific images, with no background signal. Images are readily quantified to measure apparent cell numbers at sites of accumulation. In these MRI applications, outstanding questions remain about the nature of the cellular labeling dynamics and the nanoemulsion fate over the course of labeled cell lifetime. A fluorescent, pH-sensing nanoemulsion could potentially be helpful in characterizing intracellular nanoemulsion behavior *in vitro*. More importantly, this same technology could be used for routine quantification of the degree of cell labeling of a patient’s cells *in vitro*, a parameter that is crucial for *in vivo* cell quantification from the MRI data¹⁸ and for quality control purposes. For example, a second (smaller) population of the patient’s cells could be labeled with the ratiometric nanoemulsion and the uptake could be measured using a multiwell plate reader. When in solution, the background fluorescence of CypHer5 is low, but once the nanoemulsion is consumed by cells it becomes significantly higher, and cell labeling could be monitored in real-time, without a wash step. An optical plate reader is rapid, low-cost and commonplace in biomedical and clinical laboratories, and thus is preferable over slow and more expensive ^{19}F NMR instruments, which is the current method of cell labeling assessment. Once the validated or adjusted labeling dose of fluorescent reagent is established on a small portion of the patient’s cells, the remaining therapeutic cells would be labeled

with nonfluorescent nanoemulsion and injected into the patient for *in vivo* imaging.

Information about the fate of emulsions within the cells is important to understanding the cell loading process and the stability of the probe within cells over time. For example, if the nanoemulsion enters the more acidic cellular environments, such as the lysosomal compartments, the lower pH may lead to break down of nanoemulsion components, including tracking dyes and contrast agents, leading to loss of the labels within the cells over hours or days *in vivo*. Additionally, the pH-sensing reagent can report the health of cells that have engulfed the emulsion, both *in vitro* and later *in vivo* following injection into small animals. A common uptake mechanism of nanoreagent delivery involves endocytosis,² which results in drug payload exposure to low pH in the lysosomes. The residence time of the vehicle and the drug inside lysosomes can be measured with the pH sensor incorporated into the formulation. This is important for accurate determination of intracellular localization and the nanoreagent fate. A number of pathways of internalization are known, including clathrin-mediated endocytosis, pinocytosis, phagocytosis, and micropinocytosis. Each mechanism differs in the composition of the coat, size of the isolated vesicles, and the fate of delivered substance.⁴¹ Endosomes may fuse with lysosomes or may be recycled without significant acidification to other compartments and the cell surface. Thus, development of our pH-sensing nanoemulsion may make such studies central to theranostic reagent development.

4. MATERIALS AND METHODS

Complete synthetic and experimental procedures are provided in Supporting Information.

■ ASSOCIATED CONTENT

Supporting Information

Synthetic procedures, analytical data, and experimental analyses, including formulation performance. Detailed synthesis of fluorescent reagents, PFPE oils and nanoemulsions, spectroscopy, DLS and NMR (¹H, ¹⁹F) data, and additional discussion; further experimental assessment of nanoemulsions for cell labeling applications; biological evaluation through ¹⁹F NMR and fluorescence, flow cytometry analysis, and confocal microscopy; intracellular pH measurement by flow cytometry. This information is available free of charge via the Internet at <http://pubs.acs.org/>.

■ AUTHOR INFORMATION

Corresponding Author

eta@ucsd.edu

Present Addresses

[#]Gastroenterology Department, Boston Children's Hospital, Boston, MA 02115.

[∇]Yale School of Medicine, New Haven, CT 06520.

[¶]Department of Radiology, University of California at San Diego, La Jolla, CA 92093-0695.

Notes

The authors declare no competing financial interest.

■ ACKNOWLEDGMENTS

The authors thank Kevin Hitchens, Hongyan Xu, Deepak Kadayakkara, Virgil Simplaceau, Lauren A. Ernst, Mark E. Bier, Frederick Lanni, James Fitzpatrick, and Yehuda Creeger for their valuable assistance. This work was funded by the National

Institutes of Health (P41-EB001977, P50-ES012359, R01-CA139579, U54RR02224102). NMR instrumentation at CMU was partially supported by NSF (CHE-0130903 and CHE-1039870). Mass spectroscopy instrumentation at CMU was funded by NSF (DBI-9729351).

■ REFERENCES

- (1) Godbey, W. T.; Wu, K. K.; Mikos, A. G. *J. Controlled Release* **1999**, *60*, 149.
- (2) Kaneda, M. M.; Sasaki, Y.; Lanza, G. M.; Milbrandt, J.; Wickline, S. A. *Biomaterials* **2010**, *31*, 3079.
- (3) Briggs, M. S.; Burns, D. D.; Cooper, M. E.; Gregory, S. J. *ChemComm* **2000**, 2323–2324.
- (4) Cooper, M. E.; Gregory, S.; Adie, E.; Kalinka, S. *J. Fluoresc.* **2002**, *12*, 425–429.
- (5) Barriere, H.; Lukacs, G. L. *Current Protocols in Cell Biology*; Bonifacino, J. S., Dasso, M., Eds.; John Wiley & Sons, Inc.: New York, 2008; Vol. 40, p 15.13.1–15.31.21.
- (6) Han, J.; Burgess, K. *Chem. Rev.* **2009**, *110*, 2709–2728.
- (7) Thomas, J. A.; Buchsbaum, R. N.; Zimniak, A.; Racker, E. *Biochemistry* **1979**, *18*, 2210–2218.
- (8) Schulz, A.; Hornig, S.; Liebert, T.; Birckner, E.; Heinze, T.; Mohr, G. *J. Org. Biomol. Chem.* **2009**, *7*, 1884–1889.
- (9) Mujumdar, R. B., Smith, J. A., US Patent 2000075237, 2000.
- (10) Mujumdar, R. B., Smith, J. A., EU Patent 1212375, 2002.
- (11) Mujumdar, R. B., Smith, J. A., EU Patent 1394219A1, 2004.
- (12) Johnson, I.; Spence, M. T., *The Molecular Probes Handbook: A guide to fluorescent probes and labeling technologies*; 11th ed.; Life Technologies Corporation: Carlsbad, CA, 2010, pp 66–73.
- (13) Grover, A.; Schmidt, B. F.; Salter, R. D.; Watkins, S. C.; Waggoner, A. S.; Bruchez, M. P. *Angew. Chem., Int. Ed.* **2012**, *51*, 4838–4842.
- (14) Ahrens, E. T.; Flores, R.; Xu, H. Y.; Morel, P. A. *Nat. Biotechnol.* **2005**, *23*, 983–987.
- (15) Fogel, U.; Ding, Z.; Hardung, H.; Jander, S.; Reichmann, G.; Jacoby, C.; Schubert, R.; Schrader, J. *Circulation* **2008**, *118*, 140–148.
- (16) Janjic, J. M.; Ahrens, E. T. *Wiley Interdiscip. Rev.: Nanomed. Nanobiotechnol.* **2009**, *1*, 492–501.
- (17) Kadayakkara, D. K.; Beatty, P. L.; Turner, M. S.; Janjic, J. M.; Ahrens, E. T.; Finn, O. J. *Pancreas* **2010**, *39*, 510–515.
- (18) Srinivas, M.; Morel, P. A.; Ernst, L. A.; Laidlaw, D. H.; Ahrens, E. T. *Magn. Reson. Med.* **2007**, *58*, 725–734.
- (19) O'Hanlon, C. E.; Amede, K. G.; O'Hear, M. R.; Janjic, J. M. *J. Fluorine Chem.* **2012**, *137*, 27–33.
- (20) Patel, S. K.; Zhang, Y.; Pollock, J. A.; Janjic, J. M. *PLoS ONE* **2013**, *8*, e55802.
- (21) Janjic, J. M.; Srinivas, M.; Kadayakkara, D. K.; Ahrens, E. T. *J. Am. Chem. Soc.* **2008**, *130*, 2832–2841.
- (22) Janjic, J. M., Ahrens, E. T., US Patent 8227610, 2009.
- (23) Mujumdar, R. B.; Ernst, L. A.; Mujumdar, S. R.; Lewis, C. J.; Waggoner, A. S. *Bioconjugate Chem.* **1993**, *4*, 105–111.
- (24) Zhang, W.; Curran, D. P. *Tetrahedron* **2006**, *62*, 11837–11865.
- (25) Benolken, R. M.; Emery, J. M.; Landis, D. J. *Invest. Ophthalmol.* **1974**, *13*, 71–74.
- (26) Hielscher, T. In Proceedings of European Nano Systems Conference, Paris, France, December 14–16, 2005, EDA Publishing: Cedex, France, 2005; pp 138–143.
- (27) Taurozzi, J. S.; Hackley, V. A.; Wiesner, M. R. *Preparation of nanoparticle dispersions from powdered material using ultrasonic disruption*; U.S. Department of Commerce: Washington, D.C., 2012; pp 1–15.
- (28) Jares-Erijman, E. A.; Jovin, T. M. *Nat. Biotechnol.* **2003**, *21*, 1387–1395.
- (29) Shu, D.; Zhang, H.; Petrenko, R.; Meller, J.; Guo, P. *ACS Nano* **2010**, *4*, 6843–6853.
- (30) Hitchens, T. K.; Ye, Q.; Eytan, D. F.; Janjic, J. M.; Ahrens, E. T.; Ho, C. *Magn. Reson. Med.* **2011**, *65*, 1145–1154.

- (31) Myerson, J.; He, L.; Lanza, G. M.; Tollefsen, D.; Wickline, S. J. *Thromb. Haemost.* **2011**, *9*, 1292–1300.
- (32) Pan, H.; Ivashyna, O.; Sinha, B.; Lanza, G. M.; Ratner, L.; Schlesinger, P. H.; Wickline, S. A. *Biomaterials* **2011**, *32*, 231–238.
- (33) Partlow, K. C.; Lanza, G. M.; Wickline, S. A. *Biomaterials* **2009**, *29*, 3367–3375.
- (34) Helfer, B. M.; Balducci, A.; Nelson, A. D.; Janjic, J. M.; Gil, R. R.; Kalinski, P.; De Vries, I. J. M.; Ahrens, E. T.; Mailliard, R. B. *Cytotherapy* **2010**, *12*, 238–250.
- (35) Mailliard, R. B.; Helfer, B. M.; Janjic, J. M.; Kalinski, P.; Ahrens, E. T. *J. Immunother.* **2009**, *32*, 948.
- (36) Bible, E.; Dell'acqua, F.; Solanky, B.; Balducci, A.; Crapo, P. M.; Badylak, S. F.; Ahrens, E. T.; Modo, M. *Biomaterials* **2012**, *33*, 2858–2871.
- (37) Bonetto, F.; Srinivas, M.; Heerschap, A.; Mailliard, R.; Ahrens, E. T.; Figdor, C. G.; de Vries, I. J. *Int. J. Cancer* **2011**, *129*, 365–373.
- (38) Kadayakkara, D. K. K.; Janjic, J. M.; Pusateri, L. K.; Young, W. B.; Ahrens, E. T. *Magn. Reson. Med.* **2010**, *64*, 1252–1259.
- (39) Morel, P. A.; Srinivas, M.; Turner, M. S.; Fuschiotti, P.; Munshi, R.; Bahar, I.; Feili-Hariri, M.; Ahrens, E. T. *J. Leukocyte Biol.* **2011**, *90*, 539–550.
- (40) Srinivas, M.; Turner, M. S.; Janjic, J. M.; Morel, P. A.; Laidlaw, D. H.; Ahrens, E. T. *Magn. Reson. Med.* **2009**, *62*, 747–753.
- (41) Khalil, I. A.; Kogure, K.; Akita, H.; Harashima, H. *Pharmacol. Rev.* **2006**, *58*, 32–45.